# Direct Combined ab Initio/Transition State Theory Study of the Kinetics of the Abstraction Reactions of Halogenated Methanes with Hydrogen Atoms

**Florent Louis,*,† Carlos A. Gonzalez,*,‡ and Jean-Pierre Sawerysyn†**

*Physico-Chimie des Processus de Combustion et de l'Atmosphère (PC2A) UMR CNRS 8522, FR CNRS 2416 Centre d'Etudes et de Recherche Lasers et Applications (CERLA), Université des Sciences et Technologies de Lille, 59655 Villeneuve d'Ascq Cedex, France, and Computational Chemistry Group, Physical and Chemical Properties Division, National Institute of Standards and Technology, Gaithersburg, Maryland 20899*

*Received: June 21, 2004; In Final Form: September 13, 2004*

Theoretical calculations were carried out on the H-, Cl-, and F-atom abstraction reactions from a series of seven substituted halogenated methanes ($CH_3Cl$, $CH_2Cl_2$, $CHCl_3$, $CCl_4$, $CHF_3$, $CHF_2Cl$, and $CHFCl_2$) by H atom attacks. Geometry optimizations and vibrational frequency calculations were performed using unrestricted Møller−Plesset second-order perturbation theory (UMP2) with the 6-311++G(d,p) basis set. Single-point energy calculations were performed with the highly correlated ab initio coupled cluster method in the space of single, double and triple (pertubatively) electron excitations CCSD(T) using the 6-311++G(3df,3pd) basis set. Canonical transition-state theory with a simple tunneling correction was used to predict the rate constants as a function of temperature (700−2500 K), and three-parameter Arrhenius expressions were obtained by fitting to the computed rate constants for elementary channels and overall reaction.

## I. Introduction

Model development of thermal degradation processes of halogenated compounds in flames requires detailed knowledge of the mechanisms governing such reactions as well as of the pertinent kinetic and thermodynamic data. This information is particularly invaluable in the understanding of the elementary mechanisms involved in the incineration of hazardous industrial wastes, which could aid scientists in the development of more cost effective and efficient incineration methods that will lead to more favorable environmental impacts. This is particularly true in the case of hydrogen and halogen abstraction from halogenated methanes by hydrogen atoms under combustion conditions

$$CHXYZ + H \rightarrow CXYZ + H_2 \qquad \text{(I-1)}$$

$$CHXYZ + H \rightarrow CHYZ + HX \qquad \text{(I-2)}$$

$$CHXYZ + H \rightarrow CHXZ + HY \qquad \text{(I-3)}$$

$$CHXYZ + H \rightarrow CHXY + HZ \qquad \text{(I-4)}$$

with X, Y, or Z = H, F, or Cl, which has been known to play an important role in incineration processes producing toxic materials.

One of the most difficult problems from the experimental point of view is the direct determination of the temperature dependence of the kinetics of these reactions over a temperature range wide enough to include thermal oxidation and combustion processes. Most of the time, scientists rely on extrapolations based on relatively low-temperature measurements (298−1500 K) combined with modeling in order to estimate rate constant values corresponding to combustion temperatures (1500−2500 K). However, the extrapolation procedure does not account for possible changes in the mechanisms with the temperature and tunneling effects that might significantly change as the temperature increases. In addition, most of the experimental measurements just provide overall rate constants and do not give details of the temperature dependence of the mechanisms and kinetics of the individual pathways involved in the reaction. Quantum chemical calculations in conjunction with transition state theory (TST) can help in reliably assessing the relative importance of the elementary reactions of combustion processes such as the one described in eqs I-1−I-4 without the need for empirical and complicated extrapolation procedures based on low-temperature data.

In this work, quantum chemical calculations and TST are used to compute the temperature dependence of the rate constants for the abstraction reactions by hydrogen atoms on the following series of substituted halomethanes $CH_3Cl$, $CH_2Cl_2$, $CHCl_3$, $CCl_4$, $CHF_3$, $CHF_2Cl$, and $CHFCl_2$. Direct measurements for some of these reactions have been reported in the literature.[1−11] Table 1 summarizes the available experimental results together with the corresponding references. To our knowledge, there is no experimental kinetic data for the reaction $CHFCl_2 + H \rightarrow$ products. In the case of the reaction between H-atom and the species $CHF_2Cl$ and $CHFCl_2$, no theoretical study has been reported in the literature. Berry et al.[12] reported low level calculations using the G2(MP2) and the semiempirical BAC-MP4 approach to compute rate constants in the temperature range 298−2500 K for the reaction $CHF_3 + H \rightarrow$ products. Takahashi et al.[9] performed G2(MP2) calculations adjusting the barriers to their experimental data in order to predict rate constants for all elementary reactions in the temperature range 1100−1350 K. More recently, Maity et al.[13] have applied direct dynamics calculations using canonical transition state theory and the hybrid Becke's half&half density functional theory (DFT) functional as well as the spin projected fourth order

* To whom correspondence should be addressed. Fax: (C.A.G.) (301) 869-4020. (F.L.) (33)3-20436977. E-mail: (C.A.G.) carlos.gonzalez@nist.gov; (F.L.) florent.louis@univ-lille1.fr.

† Université des Sciences et Technologies de Lille.

‡ National Institute of Standards and Technology.

10.1021/jp047305a CCC: $27.50 
Published on Web 11/03/2004

**TABLE 1: Experimental Rate Parameters for Abstraction Reaction by H Atoms from Halomethanes**

| reactant | $10^{11} \times$ A, cm$^3$.molecule$^{-1}$.s$^{-1}$ | $E_a$, kJ.mol$^{-1}$ | $k$, cm$^3$.molecule$^{-1}$.s$^{-1}$ | $T$, K | method | ref |
|---|---|---|---|---|---|---|
| $CH_3Cl$ | (15.80 ± 8.63) | 31.93 | | 870−1090 | T[a] | 1 |
| | 6.14 | 38.91 | | 500−800 | D/ESR[b] | 2 |
| | (18.30 ± 4.98) | (19.29 ± 1.35) | | 298−652 | T/ESR[c] | 3 |
| | | | $(8.00 \pm 1.99) \times 10^{-16}$ | 298 | D/ESR[b] | 4 |
| | | | $(9.30 \pm 4.65) \times 10^{-16}$ | 298 | D/MS[d] | 5 |
| | (22.40 ± 7.50) | (44.85 ± 1.68) | | 586−839 | DF/RF[e] | 6 |
| $CH_2Cl_2$ | 1.79 | 25.53 | | 298−460 | D/MS[d] | 7 |
| | (14.30 ± 5.00) | (35.33 ± 1.53) | | 491−787 | DF/RF[e] | 6 |
| $CHCl_3$ | (13.30 ± 4.30) | (30.26 ± 1.28) | | 417−854 | DF/RF[e] | 6 |
| $CCl_4$ | (13.60 ± 3.10) | (24.42 ± 0.76) | | 297−904 | DF/RF[e] | 6 |
| $CHF_3$ | 19.30 | 73.17 | | 960−1300 | T/MS [f] | 8 |
| | 15.80 | (64.60 ± 2.59) | (64.60 ± 2.59) | 1100−1350 | T/UV[g] | 9 |
| | 6.13 | 61.20 | 61.20 | 1110−1550 | T/UV[g] | 10 |
| $CHF_2Cl$ | | | $< 2.01 \times 10^{-16}$ | 298 | D/ESR[b] | 11 |
| | 77.20 | 64.27 | | 930−1160 | T/MS[f] | 8 |

[a] T: thermal. [b] D/ESR: discharge/electron spin resonance. [c] T/ESR: thermal/electron spin resonance. [d] D/MS: discharge/mass spectrometry. [e] DF/RF: discharge flow/resonance fluorescence. [f] T/MS: thermal/mass spectrometry. [g] T/UV: thermal/ultraviolet spectroscopy.

Møller−Plesset perturbation theory (PMP4) with Dunning's correlation consistent double-ζ plus polarization cc-pVDZ basis set. They reported computed rate constants in the temperature range 200−1000 K. Finally, in the case of the chloromethanes ($CH_3Cl$, $CH_2Cl_2$, $CHCl_3$, and $CCl_4$), Bryukov et al.[6] performed low level calculations of the geometries and vibrational frequencies of the stationary points using unrestricted second-order Møller−Plesset perturbation theory (UMP2) and the hybrid B3LYP DFT functionals. This information was used together with TST calculations in order to compute rate constants in the temperature range 298−3000 K. In these calculations, the reaction barriers were obtained using the Marcus equation to correlate the experimental rate constants and heats of reaction. Recently, Knyazev[14] has applied the concept of isodesmic reactions to indirectly estimate the barriers for these reactions. Rate constants computed with these barriers and TST calculations were shown to be in reasonable agreement with the experimental results reported by Bryukov et al.[6]

In this work, highly correlated ab initio quantum chemical calculations were performed in order to directly compute the reaction barriers for the title reactions without any further adjustments of the energy. The energetics of these reactions was used together with TST calculations to compute rate constants in the temperature range 300−2500 K. For all of the reactions, all possible elementary pathways are computed and their relative importance under thermal oxidation and combustion conditions (700−2500 K) are discussed. To our knowledge, this is the first time that the barriers for these reactions have been computed with highly correlated ab initio molecular orbital theory in a direct manner without recurring to empirical fitting schemes or indirect methods involving isodesmic reactions.

The remainder of this article is organized as follows. Section I (current) presents an introduction. Computational methods are reported in Section II, while the results are presented and discussed in Section III.

## II. Computational Methods[15]

Ab initio molecular orbital calculations were performed using the Gaussian 98[16] suite of programs on a 4-processor Compaq PC, 32-processor NEC SX-5, and 32-processor Silicon Graphics Origin 2000 parallel computers. All equilibrium geometries were fully optimized with the UMP2 method[17] (unrestricted second-order Møller−Plesset perturbation theory) and the 6-311++G-(d,p) basis set.[18] Harmonic vibrational frequencies of all species were calculated at the same level in order to characterize the nature of the stationary points on the potential energy surface and to compute zero-point energy corrections (used in the calculation of relative energies). Single-point energies were computed using the relatively large Pople basis set, 6-311++G-(3df,3pd),[18] and the highly correlated coupled cluster method including single and double electron excitations with triple excitations computed in a perturbative manner, CCSD(T)[19]

Canonical transition state theory[20] (TST) including semiclassical multiplicative tunneling correction factors was used to predict the temperature dependence of the rate constants. Accordingly, the rate constants, $k(T)$, were computed using the following expression:

$$k(T) = \Gamma(T) \times \frac{k_B T}{h} \times \frac{Q_{TS}(T)}{Q_H(T) Q_{halomethane}(T)} \exp\left(-\frac{E_0}{k_B T}\right) \quad \text{(II-1)}$$

where $\Gamma(T)$ indicates the transmission coefficient used for the tunneling correction at temperature $T$ and the terms $Q_{TS}(T)$, $Q_H(T)$, and $Q_{halomethane}(T)$ are the total partition functions for the transition state (TS), H atom, and halomethane, respectively, at temperature $T$. In eq II-1, the vibrationally adiabatic barrier height, $E_0$, is computed as the difference in energies between transition states and reactants, including zero-point energy corrections, $k_B$ is Boltzman's constant, and $h$ is Planck's constant.

The calculation of the reaction rate constants using the TST formulation given by eq II-1 requires the proper computation of the partition functions of reactants and the transition states. The total partition function $Q_X(T)$ of species $X$ ($X$ = H, halomethane, or TS) can be cast in terms of the translational $Q_T^X(T)$, electronic $Q_e^X(T)$, rotational $Q_R^X(T)$, and vibrational $Q_v^X(T)$ partition functions

$$Q_X(T) = Q_T^X(T) Q_e^X(T) Q_R^X(T) Q_v^X(T) \quad \text{(II-2)}$$

In this work, we adopt the simple and computationally inexpensive Wigner method[21] in the calculation of all tunneling corrections for the reactions reported here

$$\Gamma(T) = 1 + \frac{1}{24}\left(\frac{h\nu^{\neq}}{k_B T}\right)^2 \quad \text{(II-3)}$$

where $\nu^{\neq}$ is the imaginary frequency at the saddle point.

**TABLE 2: Essential Structural Parameters[a] and Imaginary Vibrational Frequencies for the Transition States of Each Reaction the MP2/6-311++G(d,p) Level of Theory**

| H atom abstraction | $r$ (C−$H_R$) | $r$ (H−$H_R$) | $\theta$ ($HH_RC$) | $L^b$ | $\nu^{\neq}$, $cm^{-1}$ |
|---|---|---|---|---|---|
| $CH_3Cl$ | 1.370 | 0.893 | 178.6 | 1.813 | 1803i |
| $CH_2Cl_2$ | 1.341 | 0.907 | 179.0 | 1.509 | 1899i |
| $CHCl_3$ | 1.318 | 0.919 | 180.0 | 1.287 | 1939i |
| $CHF_3$ | 1.410 | 0.871 | 180.0 | 2.421 | 1793i |
| $CHF_2Cl$ | 1.372 | 0.888 | 175.5 | 1.900 | 1856i |
| $CHFCl_2$ | 1.341 | 0.904 | 176.1 | 1.536 | 1905i |
| **Cl atom abstraction** | $r$ (C−$Cl_R$) | $r$ (H−$Cl_R$) | $\theta$ ($HCl_RC$) | $L^b$ | $\nu^{\ddagger}$, $cm^{-1}$ |
| $CH_3Cl$ | 1.951 | 1.563 | 180.0 | 0.600 | 1373i |
| $CH_2Cl_2$ | 1.931 | 1.588 | 176.3 | 0.519 | 1405i |
| $CHCl_3$ | 1.915 | 1.618 | 176.2 | 0.435 | 1420i |
| $CCl_4$ | 1.907 | 1.654 | 180.0 | 0.354 | 1410i |
| $CHF_2Cl$ | 1.933 | 1.563 | 176.3 | 0.617 | 1388i |
| $CHFCl_2$ | 1.921 | 1.589 | 174.1 | 0.516 | 1416i |
| **F atom abstraction** | $r$ (C−$F_R$) | $r$ (H−$F_R$) | $\theta$ ($HF_RC$) | $L^b$ | $\nu^{\ddagger}$, $cm^{-1}$ |
| $CHF_3$ | 1.665 | 1.171 | 175.8 | 1.319 | 2758i |
| $CHF_2Cl$ | 1.649 | 1.192 | 173.5 | 1.105 | 2735i |
| $CHFCl_2$ | 1.638 | 1.214 | 176.7 | 0.949 | 2690i |

[a] Bond lengths $r$ are in angstroms, and bond angles are $\theta$ in degrees; the atom involved in the abstraction is noted $X_R$ [b] The transition-state parameter $L$ is defined as the ratio of the increase in the length of the bond being broken and the elongation of the bond being formed, each with respect to its equilibrium value in the reactant and the product.

This choice seems to be appropriate to the tunneling corrections applied to rate constants at typical incineration/combustion temperatures (700−2500 K) for which the values of transmission coefficients $\Gamma(T)$ are small to moderate ($\leq 2$).[22] More sophisticated and computationally demanding algorithms such as the ones developed by Truhlar[23] and Miller[24] should be used if more accurate results are necessary. In these methods, detailed knowledge of the reaction path is needed, making the computation of tunneling corrections of relatively large electronic structure systems such as the ones containing chlorine atoms very time-consuming. In this work, rate constant calculations were performed over the temperature range of interest using the Turbo-Opt program.[25]

## III. Results and Discussion

**1. Geometric Parameters and Vibrational Frequencies.** *Geometric Parameters.* Table 2 lists the relevant structural parameters (including geometries and imaginary frequencies) calculated for the transition states. More detailed information regarding optimized geometric parameters and vibrational frequencies for reactants, transition states, and products are presented in the Tables 1S-7S of the Supporting Information.

The geometries of the transition states, predicted at the UMP2/6-311++G(d,p) level of theory, are characterized by the collinearity of the breaking C−X (X = H, F, or Cl) bond and the nascent H−X bond. The main change in the geometrical structure of the transition state can be characterized by the $L$ parameter, defined as the ratio of the increase in the length of the bond being broken and the elongation of the bond being formed.[26] This parameter provides a reliable measure of the reactant- or product-like character of the concomitant transition state. Large $L$ values correspond to product-like transition states while smaller values correspond to reactant-like TS's. The resulting values are reported in Table 2 (column 5). The observed trends in the evolution of the $L$ parameter suggest that the transition state becomes more and more reactant-like as the number of chlorine atoms in the reactant is increased in the series of chloromethanes ($CH_3Cl$, $CH_2Cl_2$, $CHCl_3$, and $CCl_4$) and fluorochloromethanes ($CHF_3$, $CHF_2Cl$, $CHFCl_2$, and $CHCl_3$). The Cl atom abstraction pathways show "early" (reactant-like) transition state structures on the potential energy surface characterized by values of $L$ smaller than 1, whereas the other pathways studied (H and F atom abstractions) are characterized by "late" (product-like) transition state structures with corresponding larger $L$ parameters.

*Vibrational Frequencies.* According to the simple Wigner tunneling formalism adopted in this work, the values of the imaginary frequencies computed for each transition state, suggest that tunneling through the barrier may be important at atmospheric temperatures ($\Gamma(T) > 2$ for $T < 700$ K). In all cases, the reaction coordinate is characterized by the migration of the abstracted atom from the carbon in the molecular substrate toward the attacking free radical hydrogen atom.

**2. Energetics and Reactivity Trends.** *Reaction Enthalpies.* Table 3 lists the reaction enthalpies ($\Delta_r H$) computed at the CCSD(T)/6-311++G(3df,3pd)//UMP2/6-311++G(d,p) level of theory for all studied abstraction channels. Calculated reaction enthalpies are very close to the literature values based on the heats of formation, $\Delta_f H°$, at 298 K of the species of interest (see Table 8S in the Supporting Information for data and relevant references) especially if the experimental uncertainties are taken into consideration. Our results show that progressive substitution of H atoms in the incipient methane moiety by chlorine atoms favors the exothermicity of the H- and Cl-abstraction reactions, whereas the substitution of chlorine by fluorine strengthens the endothermicity of the H- and F-abstraction reactions. These trends can be explained by the relatively large $\sigma$-acceptor and $\pi$-donor characters of fluorine when compared to chlorine. Accordingly, the interaction between two or more adjacent fluorine atoms stabilizes the fluoromethane, while similar interactions between chlorine atoms have a negligible stabilizing effect. In addition, geminal interactions between fluorine and chlorine atoms on the same halomethane lead to a weak stabilization.[27]

*Barrier Heights.* Table 4 shows the computed vibrationally adiabatic barriers, $E_0$, for the seven reactions under study. The following relation defines these barriers:

$$E_0 = E_{TS} - E_R + ZPE_{TS} - ZPE_R \qquad \text{(III-1)}$$

where $E_{TS}$ and $E_R$ are the computed ab initio energies of the transition state and reactants, whereas $ZPE_{TS}$ and $ZPE_R$ are their corresponding zero-point energy corrections. In the case of all of the chloromethanes, the results listed in Table 4 indicate that progressive substitution of H by Cl in the halomethane's structure tends to decrease the barrier, leading to more "reactant-like" transition structures, in keeping with Hammond's postulate.[28] However, in the case of the chlorofluoromethanes, the two effects (increasing F substitution and decreasing Cl substitution when going from $CHCl_3$ to $CHF_3$ in the series) increase the barrier height, leading to less "reactant-like" transition structures.

*Reactivity Trends: Fukui Function Analysis.* To understand the chemistry governing the trends in the potential energy barriers obtained in this work, we correlate these barriers with two highly useful reactivity indexes: Fukui functions,[29] based on the electronic structure of the reactants and the more empirical Evans−Polanyi relations which correlate barriers with heats of reactions.

**TABLE 3: Reaction Enthalpies $\Delta_r H$ Calculated at 298 K in kJ mol$^{-1}$ at CCSD(T)/6-311++G(3df,3pd)//UMP2/6-311++G(d,p) Level of Theory**

| | H abstraction | Cl abstraction | F abstraction |
|---|---|---|---|
| $H + CH_3Cl$ | −19.0(*−18.3* ± 3.8) | −85.3(*−80.9* ± 1.8) | |
| $H + CH_2Cl_2$ | −30.9(*−33.6* ± 3.8) | −102.2 (*−97.6* ± 4.0) | |
| $H + CHCl_3$ | −40.0(*−44.0* ± 3.3) | −120.2 (*−118.4* ± 3.9) | |
| $H + CCl_4$ | | −143.3(*−145.2* ± 6.6) | |
| $H + CHF_3$ | 12.6(*9.2* ± 4.2) | | −36.9 (*−37.4* ± 6.8) |
| $H + CHF_2Cl$ | −7.5(*−12.2* ± 8.0) | −71.7(*−64.5* ± 4.1) | −74.0 (*−67.5* ± 10.7) |
| $H + CHFCl_2$ | −24.3 (*−22.1* ± 19.0) | −94.5(*−86.3* ± 19.1) | −114.4 (*−117.3* ± 12.7) |

**TABLE 4: Vibrationally Adiabatic Barriers $E_0$ Calculated in KJ Mol$^{-1}$ at CCSD(T)/6-311++G(3df,3pd)//UMP2/6-311++G(d,p) Level of Theory**

| | H abstraction | Cl abstraction | F abstraction |
|---|---|---|---|
| $H + CH_3Cl$ | 46.8 | 40.3 | |
| $H + CH_2Cl_2$ | 38.2 | 36.1 | |
| $H + CHCl_3$ | 31.0 | 30.3 | |
| $H + CCl_4$ | | 23.7 | |
| $H + CHF_3$ | 60.3 | | 177.2 |
| $H + CHF_2Cl$ | 47.1 | 44.3 | 155.5 |
| $H + CHFCl_2$ | 38.0 | 36.9 | 135.7 |

The Fukui functions,[29] $f(\vec{r})$, provide a robust and efficient way to capture the physics governing chemical reactivity. Within the density functional theory (DFT) formalism, the Fukui function (FF) is defined as[29]

$$f(\vec{r}) = \left[\frac{\delta\mu}{\delta v(\vec{r})}\right]_N \qquad \text{(III-2)}$$

where $\mu$ is the chemical potential, $v(\vec{r})$ is the external potential, and $N$ is the total number of electrons. Applying Maxwell's relations of the derivatives and assuming that the total energy of a molecular system is a function of $N$, eq III-2 becomes

$$f(\vec{r}) = \left[\frac{\delta\rho}{\delta N}\right]_v \qquad \text{(III-3)}$$

where $\rho$ is the electron density. In the frozen orbital approximation,[30] the FF becomes equal to the Kohn−Sham frontier orbital density, and the following functions can be defined:[31]

$$f^{\nu}(\vec{r}) = |\phi^{\nu}(\vec{r})|^2 \qquad \text{(III-4)}$$

where $\nu$ = HOMO or LUMO and $\phi^{\nu}(\vec{r})$ is the corresponding Kohn−Sham frontier molecular orbital. When $\nu$ = HOMO (LUMO), eq III-4 quantifies the susceptibility of the molecule toward electrophilic (nucleophilic) attacks. A measure of the susceptibility toward radical attacks is given by

$$f^{\text{rad}}(\vec{r}) = \frac{(f^{\text{HOMO}}(\vec{r}) + f^{\text{LUMO}}(\vec{r}))}{2} \qquad \text{(III-5)}$$

Contreras et al.[32] have developed a method that allows their values to be computed, condensed to a particular atom $i$ on the molecule. According to this method, the condensed Fukui function at an atom $i$ is given by

$$f_i^{\nu} = \sum_{\mu\in i}^{AO}\left[|c_{\mu\nu}|^2 + c_{\mu\nu}\sum_{\kappa\neq\mu}^{\text{AO}} c_{\kappa\nu}S_{\kappa\mu}\right] \qquad \text{(III-6)}$$

where $c_{\mu\nu}$ are the molecular orbital coefficients, AO is the total number of atomic orbitals, $S_{\kappa\mu}$ is the atomic orbital overlap matrix, and $\nu$ indicates the frontier molecular orbital HOMO or LUMO as defined before. In addition, the radical Fukui function condensed to atom $i$ is given by

$$f_i^{\text{rad}} = \frac{(f_i^{\text{HOMO}} + f_i^{\text{LUMO}})}{2} \qquad \text{(III-7)}$$

**TABLE 5: Fukui Function Condensed to Atoms[a,b] and Corresponding Abstraction Classical Barriers[c]) (in kJ mol$^{-1}$) for All Halomethanes Considered in This Study**

| molecule | $f_H^{\text{rad}}$ | $f_{Cl}^{\text{rad}}$ | $f_F^{\text{rad}}$ | $E^{\dagger}_{H\_abs}$ | $E^{\dagger}_{Cl\_abs}$ | $E^{\dagger}_{F\_abs}$ |
|---|---|---|---|---|---|---|
| $CH_3Cl$ | 0.4875 | 0.7972 | | 52.7 | 41.2 | |
| $CH_2Cl_2$ | 0.3024 | 0.5013 | | 44.2 | 35.3 | |
| $CHCl_3$ | 0.0816 | 0.3538 | | 36.4 | 28.5 | |
| $CCl_4$ | | 0.2666 | | | 21.5 | |
| $CHFCl_2$ | 0.1880 | 0.4729 | 0.0113 | 43.7 | 34.9 | 133.9 |
| $CHF_2Cl$ | 0.6646 | 0.7567 | 0.0158 | 53.6 | 42.3 | 153.9 |
| $CHF_3$ | 1.2385 | | 0.1257 | 67.6 | | 176.2 |

[a] When more than one atom of the same type, an average is taken. [b] Computed at the B3LYP/6-311++G(3df,3pd)//UMP2/6-311++G(d,p) level of theory. [c] Computed at the CCSD(T)/6-311++G(3df,3pd)//UMP2/6-311++G(d,p) level of theory.

The condensed FF's have been found to be a reliable tool in the interpretation of a wide variety of problems.[33] Given that $f_i^{\text{rad}}$ provides a quantitative index of the susceptibility of atom $i$ toward radical attacks, we calculate these indices for all of the reactants treated in this study in order to provide insight in the chemistry governing the trends obtained in the computed barriers for all of the abstraction channels considered in this work. The condensed FF methodology (eqs III-6 and III-7) has been implemented in a subroutine within a modified version of the Gaussian 98 package. The Fukui functions were computed by performing single-point calculations on the geometries optimized at the UMP2/6-311++G(d,p) level of theory with the 3-parameter DFT "hybrid" exchange-correlation functional B3LYP[34] using the 6-311++G(3df,3pd) basis (B3LYP/6-311++G(3df,3pd)//UMP2/6-311++G(d,p)). Table 5 shows the results of these calculations as well as the corresponding classical barrier heights for the different abstraction channels. Analysis of the condensed FF results indicates that there is a clear correlation between the size of the Fukui function condensed to a particular atom and the corresponding barrier height for its abstraction by H atoms. Thus, the fact that chlorine abstractions exhibit lower barriers than hydrogen abstractions correlates with the larger condensed FF values for chlorine when compared to the corresponding values for hydrogen. In addition, the significantly larger barriers for fluorine abstractions correlate with its considerably lower condensed Fukui values. Overall, the results listed in Table 5 lead to the conclusion that the lower barriers observed in the case of chlorine abstractions (as compared to H- and F− abstractions) are the result of its relatively high susceptibility to attacks by radicals such as H atoms. By the same token, the significantly higher barriers in the case of F-atom abstractions are the result of its poor susceptibility to radical attacks.

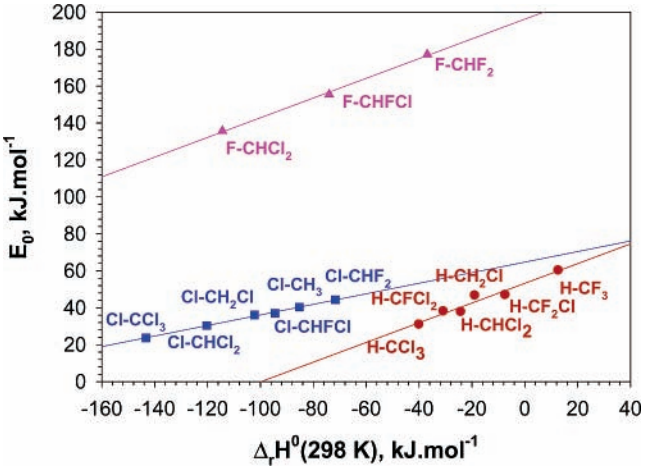


**Figure 1.** Quadratic variation of the vibrationally adiabatic barriers $E_0$ versus $\Delta_r H°$ (298 K).

*Reactivity Trends: Evans−Polanyi Relations.* Figure 1 depicts the predicted Evans−Polanyi[35] plot for all abstraction reactions considered in this study. For each type of X-abstraction channel (X = H, F, or Cl), a polynomial fit (with an $r^2$ equal to 0.99) to the data leads to the following Evans-Polanyi relation for $E_0$ (in kJ mol$^{-1}$):

$$E_0\,(\text{H-abstraction}) = -4.244 \times 10^{-4}\,\Delta_r H^2 + 0.526\,\Delta_r H + 53.33 \quad \text{(III-8)}$$

$$E_0\,(\text{Cl-abstraction}) = 2.728 \times 10^{-6}\,\Delta_r H^2 + 0.287\,\Delta_r H + 64.71 \quad \text{(III-9)}$$

$$E_0\,(\text{F-abstraction}) = 1.229 \times 10^{-3}\,\Delta_r H^2 + 0.720\,\Delta_r H + 202.10 \quad \text{(III-10)}$$

Equations III-8−III-10 show a weak quadratic behavior of the vibrationally adiabatic barriers dependence on the reaction enthalpies at 298 K, $\Delta_r H$, for the H-, Cl-, and F-abstraction channels. In principle, if information regarding the vibrationally adiabatic barrier for a similar abstraction reaction is needed, equations (III-8) − (III-10) can be used in order to predict the corresponding $E_0$ from its theoretical $\Delta_r H$ computed at the CCSD(T)/6-311++G(3df,3pd)//UMP2/6-311++G(d,p) level of theory.

**3. Kinetic Parameters Calculations.** *Rate Constants.* TST calculations using Wigner tunneling corrections were performed in order to compute reaction rate constants for each reaction channel over the temperature range 300−2500 K. For each overall reaction, the global rate constant $k(T)$ was calculated at each temperature taking into account the path degeneracy of each contributing channel. Figures 2−7 present the results of the overall rate constant calculations together with the available experimental data for comparison purposes. Overall, the results in Figures 2−7 show a marked curvature of the Arrhenius plots over the temperature range of interest, possibly as a result of tunneling effects and/or changes in the relative importance of the individual channels. With the exception of the reactions $CH_3Cl + H \rightarrow$ products and $CH_2Cl_2 + H \rightarrow$ products, excellent agreement between the computed $k(T)$'s and the experimental values is observed (Figures 4−7).

In the case of the reaction of H atoms with $CH_3Cl$, the results shown in Figure 2 and Table 2 indicate that our calculated values are in excellent agreement with the experimental results of

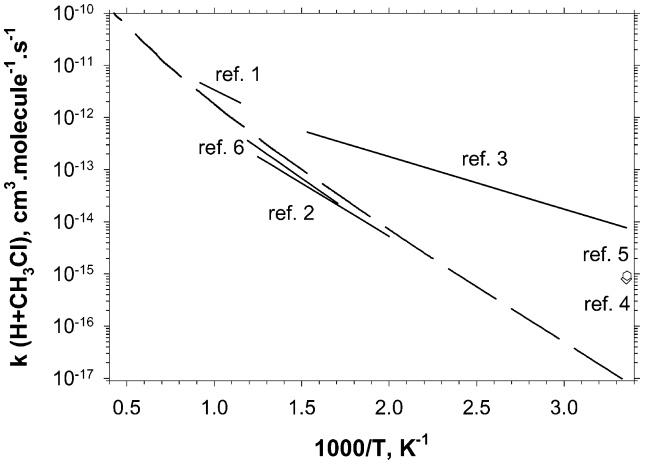


**Figure 2.** Temperature dependence of the overall rate constant of reaction H + $CH_3Cl \rightarrow$ products. Dashed line correspond to the calculated values of the rate constant at the CCSD(T)/6-311++G-(3df,3pd) level of theory.

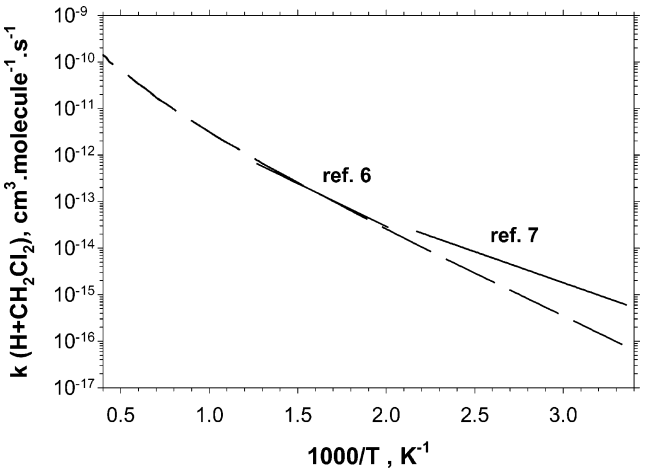


**Figure 3.** Temperature dependence of the overall rate constant of reaction H + $CH_2Cl_2 \rightarrow$ products. Dashed line correspond to the calculated values of the rate constant at the CCSD(T)/6-311++G-(3df,3pd) level of theory.

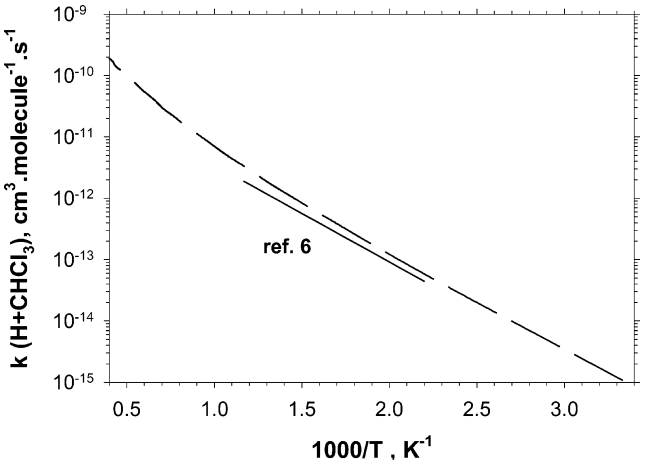


**Figure 4.** Temperature dependence of the overall rate constant of reaction H + $CHCl_3 \rightarrow$ products. Dashed line correspond to the calculated values of the rate constant at the CCSD(T)/6-311++G-(3df,3pd) level of theory.

Westenberg and DeHaas[2] as well as with the ones reported by Bryukov et al.[6] However as Figure 2 shows, our theoretical results are in significant disagreement with the temperature dependence of the experimental measurements reported in refs

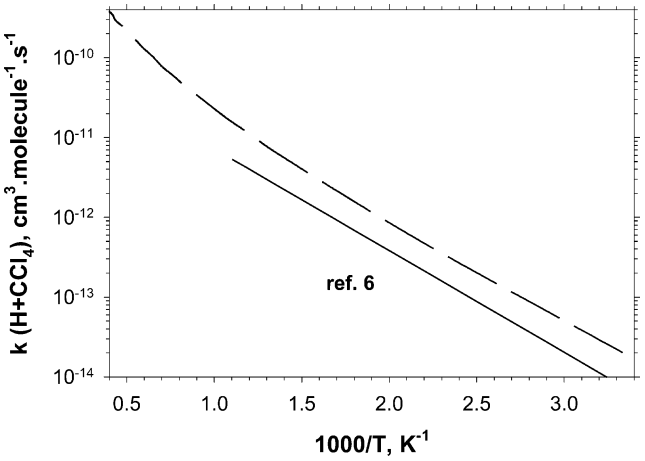


**Figure 5.** Temperature dependence of the overall rate constant of reaction H + $CCl_4$ → products. Dashed line correspond to the calculated values of the rate constant at the CCSD(T)/6-311++G(3df,3pd) level of theory.

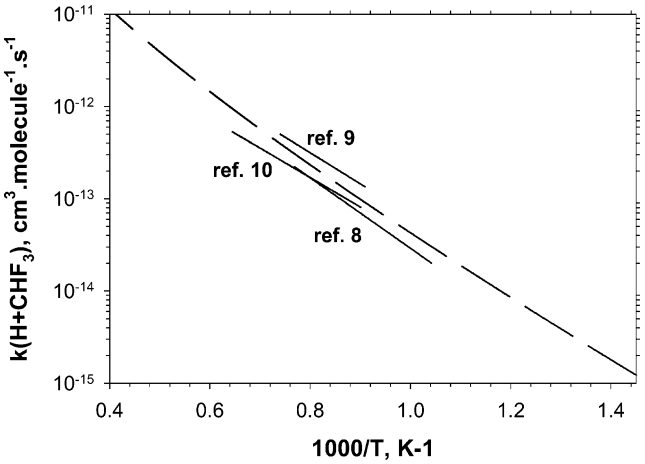


**Figure 6.** Temperature dependence of the overall rate constant of reaction H + $CHF_3$ → products. Dashed line correspond to the calculated values of the rate constant at the CCSD(T)/6-311++G-(3df,3pd) level of theory.

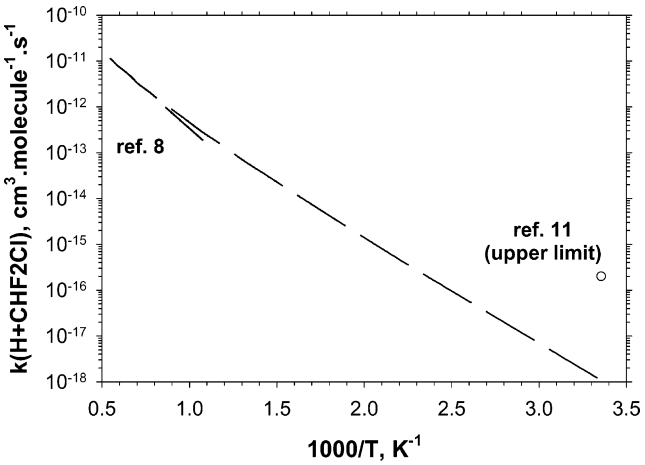


**Figure 7.** Temperature dependence of the overall rate constant of reaction H + $CHF_2Cl$ → products. Dashed line correspond to the calculated values of the rate constant at the CCSD(T)/6-311++G-(3df,3pd) level of theory.

1 and 3−5. Given the marked differences in trends shown by the experimental data, an unambiguous assessment of the quality of our theoretical predictions is difficult. However, the critical analysis of the experimental data discussed in ref 6 supporting

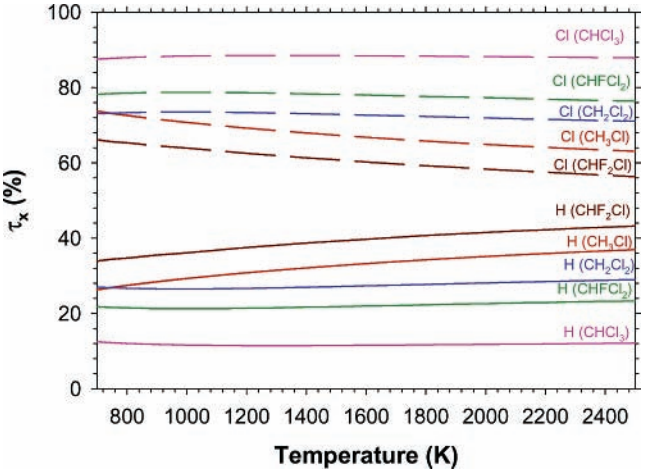


**Figure 8.** Temperature dependence of the branching ratio $\Gamma_x$ in % of H- and Cl-abstraction of the chlorine containing halomethanes.

the reliability of the results of Westenberg and DeHaas[2] as well as the ones reported by Bryukov et al.,[6] seem to provide strong arguments in favor of the validity of our theoretical predictions.

In the case of the reaction of H atoms with $CH_2Cl_2$, our calculated values are in excellent agreement with the experimental determinations (see Figure 3) of Bryukov et al.[6] At relatively low temperatures however, it is observed that the experimental rate constants obtained by Combourieu et al.[7] are consistently higher than our computed values (Figure 3) with a smaller slope in the Arrhenius plot. These discrepancies can be attributed at the interference caused by secondary reactions in the experiment that tends to consume the molecular reactant as well as H atoms, as previously discussed by Bryukov et al.[6]

Finally, the computed overall rate constants for the reaction of H atoms with $CCl_4$ were found to be systematically higher than those measured by Bryukov et al.[6] by a factor of 2.5 (Figure 5). However, over the temperature range (300−900 K), the slope ($-E_a/R$) of our predicted Arrhenius plot (−2985 K) is very close to the experimental one reported in ref 6 (−2937 K).

*Branching Ratios.* For an abstraction reaction by H atom and a molecule *M*, we define the branching ratio $\tau_X^M$ (in %) as the ratio of the rate constant for the X-abstraction pathway to that of the overall rate constant of the reaction. For example, in the case of the $CHF_2Cl$, the branching ratio for the H-abstraction channel is given by the following equation:

$$\tau_{\mathrm{H}}^{\mathrm{CHF_2Cl}}(T) = \frac{k_{\mathrm{H}}^{\mathrm{CHF_2Cl}}(T)}{k_{\mathrm{H}}^{\mathrm{CHF_2Cl}}(T) + k_{\mathrm{Cl}}^{\mathrm{CHF_2Cl}}(T) + k_{\mathrm{F}}^{\mathrm{CHF_2Cl}}(T)} \times 100\% \qquad \text{(III-11)}$$

where $k_{\mathrm{H}}^{\mathrm{CHF_2Cl}}(T)$, $k_{\mathrm{Cl}}^{\mathrm{CHF_2Cl}}(T)$, and $k_{\mathrm{F}}^{\mathrm{CHF_2Cl}}(T)$ are the rate constants for the H-, Cl-, and F-abstraction channels at temperature *T* respectively. The branching ratios of H-, Cl-, and F-abstraction channels calculated over the temperature range (700−2500 K) are reported in Table 9S of the Supporting Information. The results of these calculations are summarized in graphical form in Figure 8, where the temperature-dependence of the branching ratios of the relevant channels (H- and Cl-abstraction) is depicted. At typical incineration/combustion temperatures, we found that the F-abstractions exhibit very low $\tau_{\mathrm{F}}^{\mathrm{M}}$ values (at most 1% at 2500 K) indicating that they are not competitive with the other abstraction channels in the consumption of the parent halomethane undergoing thermal degradation. For all the studied species, Cl-abstraction is consistently the most important channel over the whole temperature range. The results indicate

**TABLE 6: Summary of the Arrhenius Parameters of Elementary Channels Calculated over the Temperature Range 700−2500 K**

| | H abstraction | | | Cl abstraction | | | F abstraction | | |
|---|---|---|---|---|---|---|---|---|---|
| | $B^a$ | $n$ | $E_a/R$ (K) | $B^a$ | $n$ | $E_a/R$ (K) | $B^a$ | $n$ | $E_a/R$ (K) |
| $H + CH_3Cl$ | $2.5 \times 10^{-17}$ | 2.073 | 4370 | $6.1 \times 10^{-16}$ | 1.731 | 4315 | | | |
| $H + CH_2Cl_2$ | $1.5 \times 10^{-17}$ | 2.068 | 3325 | $7.7 \times 10^{-16}$ | 1.693 | 3690 | | | |
| $H + CHCl_3$ | $7.7 \times 10^{-18}$ | 2.033 | 2460 | $1.2 \times 10^{-15}$ | 1.664 | 2945 | | | |
| $H + CCl_4$ | | | | $2.6 \times 10^{-15}$ | 1.632 | 2185 | | | |
| $H + CHF_3$ | $1.3 \times 10^{-17}$ | 2.062 | 6190 | | | | $3.5 \times 10^{-16}$ | 1.769 | 20030 |
| $H + CHF_2Cl$ | $1.1 \times 10^{-17}$ | 2.050 | 4520 | $3.1 \times 10^{-16}$ | 1.661 | 4605 | $2.3 \times 10^{-16}$ | 1.748 | 17420 |
| $H + CHFCl_2$ | $9.4 \times 10^{-18}$ | 2.030 | 3345 | $6.5 \times 10^{-16}$ | 1.658 | 3715 | $1.2 \times 10^{-16}$ | 1.745 | 15050 |

[a] Units in $cm^3$ $molecule^{-1}$ $s^{-1}$

**TABLE 7: Summary of the Arrhenius Parameters of Overall Reaction Calculated over the Temperature Range 700−2500 K**

| | $B^a$ | $n$ | $E_a/R$ (K) |
|---|---|---|---|
| $H + CH_3Cl$ | $3.6 \times 10^{-16}$ | 1.859 | 4305 |
| $H + CH_2Cl_2$ | $4.8 \times 10^{-16}$ | 1.794 | 3590 |
| $H + CHCl_3$ | $1.1 \times 10^{-15}$ | 1.696 | 2905 |
| $H + CCl_4$ | $2.6 \times 10^{-15}$ | 1.632 | 2185 |
| $H + CHF_3$ | $1.1 \times 10^{-17}$ | 2.090 | 6160 |
| $H + CHF_2Cl$ | $1.2 \times 10^{-16}$ | 1.849 | 4525 |
| $H + CHFCl_2$ | $4.0 \times 10^{-16}$ | 1.750 | 3625 |

[a] Units in $cm^3$ $molecule^{-1}$ $s^{-1}$.

that progressive substitution of H or F by Cl in the series of halomethanes considered in this study tends to increase the branching ratio $\tau_{Cl}^{M}$. These trends are in accord with the results of the Fukui function analysis discussed above.

*Arrhenius Parameters.* The modified three-parameter Arrhenius expression $k(T) = BT^n \exp(-E_a/RT)$ fitted to each elementary and overall rate constant computed over the temperature range 700−2500 K is reported in Tables 6 and 7. Given the excellent agreement with the experimental rate constants (see Rate Constants section above), we recommend the Arrhenius parameters computed with our highly correlated method for use in the modeling of thermal degradation and combustion processes involving the abstraction reactions discussed in this work. In addition, this excellent agreement gives us confidence in our predicted kinetic parameters in the case of the $H + CHFCl_2$ reaction for which no experimental data is available.

## Conclusion

High-correlated ab initio electronic structure calculations, combined with canonical Transition State Theory, were performed on the reactions of H atoms with a series of substituted halogenated methanes. Computed rate constants as well as electronic structure analysis based on Fukui functions condensed to atoms lead to the conclusion that the Cl- and H-abstraction channels are important at typical incineration/combustion temperatures with the Cl-abstraction being the major channel. It was found that this result holds regardless of the number of chlorine atoms in the parent halomethane. In addition, it is found that overall rate constants computed at the CCSD(T)/6-311++G(3df,3pd)//UMP2/6-311++G(d,p) level of theory are in excellent agreement with their corresponding experimental counterparts.

**Acknowledgment.** The authors thank the CERLA and the "Institut du Développement et des Ressources en Informatique Scientifique" (IDRIS) for providing computing time for part of the theoretical calculations under projects MUST and 20042. We are also grateful to the "Ministère de la Recherche et de l'Enseignement Supérieur", the "Région Nord/Pas de Calais", and the "Fonds Européen de Développement Economique des Régions" (FEDER) for partial funding of this work and for supporting CERLA. The authors would also like to thank Dr. Denis Lehane for his invaluable help with the computations performed in Central Computer Facilities at NIST and Dr. Yamil Simon-Manso (CSTL, NIST) for fruitful discussions.

**Supporting Information Available:** Computed optimized geometry parameters and vibrational frequencies for all reactants, transition structures, and products considered in this study. The literature values of the heat of formation corresponding to the reactants and products under study as well as the branching ratio of H-, Cl-, and F-abstraction channels as a function of the temperature are also listed. This material is available free of charge via the Internet at http://pubs.acs.org.

## References and Notes

(1) Hart, L. W.; Grunfelder, C.; Fristrom, R. M. *Combust. Flame* **1974**, *23*, 109.
(2) Westenberg, A. A.; deHaas, N. *J. Chem. Phys.* **1975**, *62*, 3321.
(3) Aders, W.-K.; Pangritz, D.; Wagner, H. Gg. *Ber. Bunsen-Ges. Phys. Chem.* **1975**, *79*, 90.
(4) Jones, W. E.; Ma, J. L. *Can. J. Chem.* **1986**, *64*, 2192.
(5) Triebert, J.; Meinike, T.; Olzmann, M.; Scherzer, K. *Z. Phys. Chem.* **1995**, *191*, 47.
(6) Bryukov, M. G.; Slagle, I. R.; Knyazev, V. D. *J. Phys. Chem. A* **2001**, *105*, 3107.
(7) Combourieu, J.; Le Bras, G.; Paty, C. *Symp. Int. Comb. Proc.* **1973**, *14*, 485.
(8) Richter, H.; Vandooren, J.; Van Tiggelen, P. J. *J. Chim. Phys.* **1994**, *91*, 1748.
(9) Takahashi, K.; Yamamori, Y.; Inomata, T. *J. Phys. Chem. A* **1997**, *101*, 9105.
(10) Hranisavljevic, J.; Michael, J. V. *J. Phys. Chem. A* **1998**, *102*, 7668.
(11) Egorov, V. I.; Temchin, S. M.; Gorban, N. I.; Balakhnin, V. P. *Kinet. Catal.* **1979**, *20*, 850.
(12) Berry, R. J.; Ehlers, C. J.; Burgess, D. R., Jr.; Zachariah, M. R.; Marshall, P. *Chem. Phys. Lett.* **1997**, *269*, 107.
(13) Maity, D. K.; Duncan, W. T.; Truong, T. N. *J. Phys. Chem. A* **1999**, *103*, 2152.
(14) Knyazev, V. D. *J. Phys. Chem. A.* **2002**, *106*, 11603.
(15) The identification of commercial equipment or materials does not imply recognition or endorsement by the National Institute of Standards and Technology, nor does it imply that the material or equipment identified are necessarily the best available for the purpose.
(16) Frisch, M. J.; Trucks, G. W.; Schlegel, H. B.; Scuseria, G. E.; Robb, M. A.; Cheeseman, J. R.; Zakrzewski, V. G.; Montgomery, J. A., Jr.; Stratmann, R. E.; Burant, J. C.; Dapprich, S.; Millam, J. M.; Daniels, A. D.; Kudin, K. N.; Strain, M. C.; Farkas, O.; Tomasi, J.; Barone, V.; Cossi, M.; Cammi, R.; Mennucci, B.; Pomelli, C.; Adamo, C.; Clifford, S.; Ochterski, J.; Petersson, G. A.; Ayala, P. Y.; Cui, Q.; Morokuma, K.; Malick, D. K.; Rabuck, A. D.; Raghavachari, K.; Foresman, J. B.; Cioslowski, J.; Ortiz, J. V.; Stefanov, B. B.; Liu, G.; Liashenko, A.; Piskorz, P.; Komaromi, I.; Gomperts, R.; Martin, R. L.; Fox, D. J.; Keith, T.; Al-Laham, M. A.; Peng, C. Y.; Nanayakkara, A.; Gonzalez, C.; Challacombe, M.; Gill, P. M. W.; Johnson, B. G.; Chen, W.; Wong, M. W.; Andres, J. L.; Head-Gordon, M.; Replogle, E. S.; Pople, J. A. *Gaussian 98*, revision A.7; Gaussian, Inc.: Pittsburgh, PA, 1998.
(17) Møller, C.; Plesset, M. S. *Phys. Rev.* **1934**, *46*, 618.
(18) Descriptions of the Pople-style basis sets can be found in the following: Foresman, J. B.; Frisch, A. E. *Exploring Chemistry with Electronic Structure Methods*, 2nd ed.; Gaussian, Inc.: Pittsburgh, PA, 1996.

(19) (a) Bartlett, R. J.; Purvis, G. D. *Int. J. Quantum. Chem.* **1978**, *14*, 516. (b) Cizek, J. *Adv. Chem. Phys.* **1969**, *14*, 35. (c) Purvis, G. D.; Bartlett, R. J. *J. Phys. Chem.* **1982**, *76*, 1910. (d) Scuseira, G. E.; Janssen, C. L.; Schaefer, H. F., III. *J. Chem. Phys.* **1988**, *89*, 7382. (e) Scuseira, G. E.; Schaefer, H. F., III. *J. Chem. Phys.* **1989**, *90*, 3700. (f) Pople, J. A.; Head-Gordon, M.; Raghavachari, K. *J. Chem. Phys.* **1987**, *87*, 5968.

(20) (a) Johnston, H. S. *Gas-Phase Reaction Rate Theory*; The Roland Press Company: New York, 1966. (b) Laidler, K. J. *Theories of Chemical Reaction Rates*; McGraw-Hill: New York, 1969. (c) Weston, R. E.; Schwartz, H. A. *Chemical Kinetics*; Prentice Hall: New York, 1972. (d) Rapp, D. *Statistical Mechanics*; Holt, Reinhard, and Winston: New York, 1972. (e) Nikitin, E. E. *Theory of Elementary Atomic and Molecular Processes in Gases*; Claredon Press: Oxford, U.K., 1974. (f) Smith, I. W. M. *Kinetics and Dynamics of Elementary Gas Reactions*; Butterworth: London, 1980. (g) Steinfeld, J. I.; Francisco, J. S.; Hase, W. L. *Chemical Kinetics and Dynamics*; Prentice Hall: New Jersey, 1989.

(21) Wigner, E. P. *Z. Phys. Chem*. **1932**, *B19*, 203.

(22) Bell, R. P. *The Tunnel Effect in Chemistry*; Chapman and Hall: New York, 1980.

(23) (a) Garret, B. C.; Truhlar, D. G. *J. Phys. Chem*. **1979**, *83*, 2921. (b) Garret, B. C.; Truhlar, D. G. *J. Chem. Phys*. **1984**, *81*, 309. (c) Skodke, R. T.; Garret, B. C.; Truhlar, D. G. *J. Phys. Chem*. **1981**, *85*, 3019. (d) Skodje, R. T.; Garret, B. C.; Truhlar, D. G. *J. Chem. Phys.* **1982**, *77*, 5955. (e) Garret, B. C.; Truhlar, D. G.; Grev, R. S. Magnuson, A. W. *J. Chem. Phys.* **1980**, *84*, 1730. (f) Garret, B. C.; Truhlar, D. G.; Grev, R. S. Magnuson, A. W. *J. Chem. Phys.* **1983**, *87*, 4554.

(24) (a) Miller, W. H.; Shi, S.-h. *J. Chem. Phys*. **1981**, *75*, 2258. (b) Miller, W. H.; Smith, F. T. *Phys. Rev*. **1978**, *A 17*, 939.

(25) Rate constants calculated with the Turbo-Rate module in the beta version of the TURBO−OPT geometry optimization package, developed by C. Gonzalez and T. Allison, National Institute of Standards and Technology, Gaithersburg, MD.

(26) Rayez, M.-T.; Rayez, J.-C.; Sawerysyn, J. P. *J. Phys. Chem.* **1994**, *98*, 11342.

(27) (a) Rodriquez, C. F.; Sirois, S.; Hopkinson, A. C. *J. Org. Chem.* **1992**, *57*, 4869. (b) *Organofluorine Chemistry: Principles and Commercial Applications*; Banks, R. E., Smart, B. E., Tatlow, J. C., Eds.; Plenum Press: New York, 1994.

(28) Hammond, G. S. *J. Am. Chem. Soc*. **1955**, *77*, 334.

(29) (a) Parr, R. G.; Yang, W. *Density Functional Theory of Atoms and Molecules*; Oxford University Press: New York, 1989. (b) Parr, R. G.; Yang, W. *J. Am. Chem. Soc*. **1984**, *106*, 4049. (c) Yang, W.; Parr, R. G.; Pucci, R. *J. Chem. Phys*. **1984**, *81*, 2862. (d) Yang, W.; Parr, R. G. *Proc. Natl. Acad. Sci. U.S.A.* **1985**, *82*, 6723.

(30) Ciosloski, J.; Martinov, M.; Mixon, S. T. *J. Phys. Chem*. **1993**, *97*, 10948.

(31) Senet, P. *J. Chem. Phys*. **1997**, *107*, 2516.

(32) Contreras, R. R.; Fuentealba, P.; Galván, M.; Pérez, P. *Chem. Phys. Lett*. **1999**, *304*, 405.

(33) See for example: (a) Fuentealba, P.; Contreras, R. R. In *Reviews of Modern Quantum Chemistry. A Celebration of the Contributions of Robert G Parr*; World Scientific: Singapore, 2002; p 1013. (b) Chermette, H.; Boulet, P.; Portmann, S. In *Reviews of Modern Quantum Chemistry. A Celebration of the Contributions of Robert G Parr*; World Scientific: Singapore, 2002; p 992. (c) Fuentealba, P.; Pérez, P.; Contreras, R. R. *J. Chem. Phys*. **2000**, *113*, 2544. (d) Bulat, F. A.; Chamorro, E.; Fuentealba, P.; Toro-Labbé *J. Phys. Chem. A* **2004**, *108*, 342.

(34) Becke, A. D. *J. Chem. Phys*. **1996**, *104*, 1040.

(35) (a) Bell, R. P. *Proc. R Soc. London Ser. A* **1936**, *154*, 414. (b) Bell, R. P.; Lidwell, O. M. *Proc. R Soc. London Ser. A* **1940**, *176*, 114. (c) Ogg, R. A., Jr.; Polanyi, M. *Trans Faraday Soc.* **1935**, *31*, 604. (d) Evans, M. G.; Polanyi, M. *Trans Faraday Soc.* **1935**, *31*, 875. (e) Evans, M. G.; Polanyi, M. *Trans Faraday Soc.* **1936**, *32*, 1333. (f) Evans, M. G. *Trans. Faraday Soc.* **1946**, *42*, 719.